Received: 4 September 2023 | Revised: 29 November 2023 | Accepted: 8 January 2024

DOI: 10.4218/etrij.2023-0367

ORIGINAL ARTICLE

ETRI Journal WILEY

Moment analysis on channel eigenvalue for DAS-to-DAS system

Donghyuk Gwak[1] | **Youngil Jeon**[2] | **Jemin Lee**[3] | **Jee-Hyeon Na**[1]

[1]Mobile Communication Research Division, Electronics and Telecommunications Research Institute, Daejeon, Republic of Korea

[2]Satellite Communication Research Division, Electronics and Telecommunications Research Institute, Daejeon, Republic of Korea

[3]School of Electrical and Electronic Engineering, Yonsei University, Seoul, Republic of Korea

Correspondence
Jee-Hyeon Na, Mobile Communication Research Division, Electronics and Telecommunications Research Institute, Daejeon, Republic of Korea.
Email: jhna@etri.re.kr

Funding information
This work was supported by Institute of Information & communications Technology Planning & Evaluation (IITP) grant funded by the Korea government (MSIT) (No. 2018-0-01659, 5G Open Intelligence-Defined RAN (ID-RAN) Technique based on 5G New Radio)

Abstract

In this paper, we study on channel eigenvalue distribution of MIMO system, namely, DAS-to-DAS system, of which transmit and receive nodes are geometrically distributed in unplanned manner. It offers key to performance upper bound analysis of collaborative transmission in unplanned network and multi-user transmission of distributed antenna system. Previous studies on stochastic geometry have analyzed performance of single typical receiver, while transmitters are geometrically distributed. And random matrix theory has unveiled probabilistic behavior of MIMO channel eigenvalues, while transmit and receive antennas are collocated. Our study integrates knowledge from the two different research fields to extend the applicability to analysis on channel eigenvalue distribution of DAS-to-DAS system. As a preliminary research on such channel eigenvalue distribution, its first few moments are derived in analytic form. And its coherency of the analysis results with Monte-Carlo simulation results has examined.

KEYWORDS

DAS, DAS to DAS, moment analysis, random matrix theory, unplanned network

1 | INTRODUCTION

As the traffic demand per area soaring higher, ultra-dense network has been suggested as a proper remedy to satisfy such demand. And the scaling laws of cellular networks offer theoretical support for such solution. The studies on trend of area spectral efficiency over increasing base station density are well established on both scenarios of regularly and irregularly deployed base stations. Recent works [1] have extended the literature to point-to-point MIMO transmission under irregularly deployed base station scenario. However, those works focus on single-stream transmission performance of MIMO channel between one collocated antenna group and one scattered antenna group.

The nature of unplanned network is often represented as distributed antenna system (DAS) and modeled with point Poisson process (PPP) [2]. The assumption of stochastically distributed nodes is perceived as fairly general and also convincing since it reflects non-ideal geometric features of realistic cellular network deployment. And DAS has also been introduced in describing systems with scattered mobile stations or ad hoc nodes. The state-of-art studies on scattered base stations have

been extended to cooperative transmission [3], while those on scattered mobile stations have been extended to analysis of non-orthogonal multiple access (NOMA) application [4].

One step further from DAS, we are newly suggesting a system consisting of two groups of mutually independently scattered nodes, and we have denominated such a system as DAS-to-DAS. The analysis on multi-stream performance of DAS to DAS is challenging, since nodes of both groups are geometrically scattered and there is no existing methodology providing a mean to deal with such MIMO channel. Furthermore, the basic assumption of DAS to DAS that the both groups equip infinite number of nodes implies that the channel matrix is of doubly infinite dimension, which is challenging to deal with. We have devised a novel methodology that is largely inspired by knowledge of random matrix theory (RMT), which is frequently applied on analysis of doubly infinite channel matrix.

The progresses in RMT [5–8] have been imported to wireless communication research providing means to access profound understanding on probabilistic behavior of multi-stream MIMO system performance. Unlike typical assumption of DAS studies, the system models that RMT concerns commonly assume multiple nodes for both of transmitter and receiver side. RMT has enabled to obtain eigenvalue distributions of random matrices in analytic form, while its application is limited only on a number of generic random matrix groups. The probabilistic distribution of eigenvalues can be utilized in calculating a variety of system performance measures of MIMO system. However, the application of RMT has been limited to point-to-point transmission scenario where transmit nodes and receive nodes are, respectively, collocated. Because, it is required to control the pathloss factor of every transmit and receive antenna pair to be all identical in order to obtain a channel matrix in RMT applicable form.

In this paper, the forementioned two theories are combined to unveil probabilistic profile of eigenvalues for MIMO channel matrix between two node groups geometrically distributed. The random entities of the channel matrix are modeled by exploiting PPP with consideration of both of geometric and fading factor. And apporoaches of RMT have been adopted to obtain closed form solution for moments of eigenvalues of the channel matrix. Since a probability density function can be reconstructed with the knowledge of moments of all order, the full probabilistic profile of DAS-to-DAS MIMO channel eigenvalues can be obtained from it.

The ultimated goal of this work is to enable per-area capacity analysis of DAS to DAS consisting of numberless nodes over infinite plane. The accurate per-area capacity analysis can be conducted only with the knowledge of probability density function of channel matrix eigenvalues. However, lower bound analysis that requires partial knowledge on moments of channel matrix eigenvalues has been conducted and presented in this paper.

2 | SYSTEM MODEL

We consider a MIMO system consisting of geometrically scattered transmit (Tx) and receive (Rx) nodes, and all nodes are assumed to be equipped with single antenna. The geometric distribution of Tx nodes and Rx nodes are, respectively, represented by two mutually independent homogeneous Poisson point processes (PPP) defined over $\mathbb{R}^2$ plain. Each channel coefficient representing pairwise channel between a Tx node and an Rx node is modeled with regarding pathloss and Rayleigh fading factors only.

2.1 | Geometric distribution of nodes

Let $\mathbf{p}_j$ and $\mathbf{q}_i$, respectively, be the positions of the jth Tx node and the ith Rx node. The PPP Φ_t represents the distribution of Tx nodes $\Phi_t = \sum_j \delta\left(\mathbf{x} - \mathbf{p}_j\right)$, and the PPP Φ_r is that of Rx nodes $\Phi_r = \sum_i \delta(\mathbf{x} - \mathbf{q}_i)$ with the definition of Dirac delta function $\delta(\mathbf{x})$. Assume PPPs Φ_t and Φ_r have homogeneity feature that their intensities ρ_t and ρ_r with unit of nodes/m^2 are uniform over the whole $\mathbb{R}^2$ plain.

2.2 | Pathloss models

To prevent the pathloss value to diverge to infinity as inter-node distance approaches to zero, non-singular pathloss models are exploited. Among widely accepted pathloss models, two non-singular pathloss models are chosen for exemplification. One is minimum spacing pathloss model (MSPM) [9], which sets virtual minimum distance and its pathloss function over distance $L(d)$ is defined as

$$L(d) = \sqrt{c_0}\max(d, d_0)^{-\alpha/2}, \tag{1}$$

where c_0 is reference power gain, d is inter-node distance, d_0 is virtual minimum distance, and α is pathloss exponent. And the other one is the vertical elevation pathloss model (VEPM) [10], which sets height difference between transmitters and receivers and its pathloss function is defined as

$$L(d) = \sqrt{c_0}\sqrt{h_0^2 + d^2}^{-\alpha/2}, \tag{2}$$

where h_0 is relative vertical elevation of transmitters. Note that any generic pathloss model can substitute the

exemplified pathloss models for the analysis conducted throughout the paper as long as its pathloss function satisfies the conditions that $\int_0^\infty L^{2k}(r)2\pi r dr < \infty$ for arbitrary $k \in \mathbb{N}$.

2.3 | Channel matrix generation

Denote by $\mathbf{H} \in \mathbb{C}^{\infty \times \infty}$ the channel matrix between the Tx nodes and the Rx nodes. The propagation channel gain between the ith Rx node and the jth Tx node h_{ij} is modeled with the consideration of pathloss and Rayleigh fading. Thus, h_{ij} can be presented as $h_{ij} = g_{ij}\beta_{ij}$ where g_{ij} is Rayleigh fading coefficient, which follows the distribution of $\mathcal{CN}(0, 1^2)$, and β_{ij} is the distance-dependent pathloss attenuation.

The pathloss attenuation β_{ij} is determined by the distance between the ith Rx node and the jth Tx node d_{ij} with the pathloss function $L(\cdot)$ as $\beta_{ij} = L(d_{ij})$. We further assume that $\{d_{ij}, g_{ij}\}_{i,j \in \mathbb{N}}$ are mutually independent.*

3 | MOMENT ANALYSIS ON CHANNEL EIGENVALUES

3.1 | Channel eigenvalues and their moments

Let $\mathbf{W}$ be the squared channel matrix by forming a Gramian matrix made up from the column vectors of $\mathbf{H}$ (or alternatively $\mathbf{H}^H$ in case of $\rho_t \le \rho_r$)

$$\mathbf{W} = \begin{cases} \mathbf{H}^H\mathbf{H} & (\text{for } \rho_t \le \rho_r) \\ \mathbf{H}\mathbf{H}^H & (\text{for } \rho_t > \rho_r) \end{cases}. \tag{3}$$

We take $\mathbf{W} = \mathbf{H}\mathbf{H}^H$ case without loss of generality and form a compact squared matrix in order to avoid redundant zero eigenvalues. The eigenvalues of $\mathbf{W}$ are denoted by $\{\lambda_n\}_{n=1}^{\infty}$, which are referred as channel eigenvalues of $\mathbf{H}$.

The moments of its channel eigenvalues are studied in order to investigate the properties of the channel matrix $\mathbf{H}$. Since the value of its trace is equal to the sum of its eigenvalues, we have equation of $\mathrm{Tr}(\mathbf{W}) = \sum_n \lambda_n$ and expand it to arbitrary powers of the matrix as

$$\mathrm{Tr}(\mathbf{W}^k) = \sum_i [\mathbf{W}^k]_{ii} = \sum_n \lambda_n^k. \tag{4}$$

By exploiting the probability density identity property among the eigenvalues and among the diagonal entries of $\mathbf{W}$, which roots on symmetricity, we can drop off summation in 4 by dividing both side with n. Let λ be a random variable following distribution of eigenvalue λ_n, which has identical distribution regardless over any n. As result, we can present the kth moment of λ, namely, μ_k, as

$$\mu_k := \mathbb{E}[\lambda^k] = \mathbb{E}[[\mathbf{W}^k]_{ii}]. \tag{5}$$

The entries of $\mathbf{W}^k$ can be obtained by the rule of matrix chain multiplication (such as $[\mathbf{ABC}]_{ps} = \sum_{q,r} a_{pq} b_{qr} c_{rs}$)

$$[\mathbf{W}^k]_{ij} = \sum_{\substack{\mathbf{u} \in \mathbb{N}^{2k+1} \\ u_1 = i \\ u_{2k+1} = j}} \mathcal{E}(\mathbf{H}, \mathbf{u}, k), \tag{6}$$

where $\mathbf{u} = [i_1, j_1, i_2, j_2, \ldots, i_k, j_k, i_{k+1}]^\top$ is an alternating sequence of row indices and column indices of $\mathbf{W}$ and its corresponding chain product is

$$\mathcal{E}(\mathbf{H}, \mathbf{u}, k) := \prod_{l=1}^{k} h_{u_{2l-1}u_{2l}} h^*_{u_{2l+1}u_{2l}}. \tag{7}$$

Then, μ_k can be calculated by

$$\mu_k = \sum_{\substack{\mathbf{u} \in \mathbb{N}^{2k+1} \\ u_1 = u_{2k+1} = i}} \mathcal{E}(\mathbf{H}, \mathbf{u}), \tag{8}$$

where $\Pi(\mathbf{H}, \mathbf{u}) = \mathbb{E}[\mathcal{E}(\mathbf{H}, \mathbf{u}, k)]$.

3.2 | Classification of sequences and sequence group naming convention

Let us define counting functions $\psi_{\mathbf{u}}(i,j)$ and $\phi_{\mathbf{u}}(i,j)$ as the number of appearances of h_{ij} and h^*_{ij} in the chain product $\mathcal{E}(\mathbf{H}, \mathbf{u}, k)$, respectively. Then, the chain product in (7) can be converted into a concise form as

$$\mathcal{E}(\mathbf{H}, \mathbf{u}, k) = \prod_{(i,j)} h_{ij}^{\psi_{\mathbf{u}}(i,j)} \prod_{(i,j)} h_{ij}^{*\phi_{\mathbf{u}}(i,j)}. \tag{9}$$

*Note that the assumption does not hold in strict sense since the high-order statistics of $\{d_{ij}\}_{i,j \in \mathbb{N}}$ have weak but still existing dependency. However, the dependency leaves insignificant level of error that we take the assumption to be valid.

In (8), the summation is performed over all possible index sequences of $\mathbf{u} \in \mathbb{N}^{2k+1}$ for given k, which have starting and ending indices are identical to i. Since the resultant values that $\Pi(\mathbf{H}, \mathbf{u})$ can be are not diverse as the index sequences themselves are, thus, the whole set of index sequences can be classified into several groups sharing an identical $\Pi(\mathbf{H}, \mathbf{u})$ value within each group. First, we denote the biggest sequence group which outputs $\Pi(\mathbf{H}, \mathbf{u}) = 0$ as "nil sequence group," and the common necessary condition to meet to be a nil sequence is described in the following lemma.

Lemma 1 (Nil sequence condition). $\Pi(\mathbf{H}, \mathbf{u}) = 0$ always holds true if $\mathbf{u}$ includes any pair (i,j), which does not satisfy $\psi_{\mathbf{u}}(i,j) = \phi_{\mathbf{u}}(i,j)$.

Proof. Let there exists any (i,j) that $\psi_{\mathbf{u}}(i,j) - \phi_{\mathbf{u}}(i,j) > 0$. Then, the condition given implies that the chain product contains non-zero power of g_{ij}, which is unmatched with the equivalent power of its conjugate g_{ij}^*. Since g_{ij} is complex Gaussian random variable with circular symmetric distribution and is independent to any element of $\left\{g_{i'j'}, g_{i'j'}^*, \beta_{i'j'}\right\}_{i',j' \in \mathbb{N}, (i',j') \neq (i,j)}$ and also β_{ij}, $\mathbb{E}\left[g_{ij}^{\psi_{\mathbf{u}}(i,j)} - \phi_{\mathbf{u}}(i,j)\right] = 0$.

$$\Pi(\mathbf{H},\mathbf{u}) = \mathbb{E}\left[g_{ij}^{\psi_{\mathbf{u}}(i,j)-\phi_{\mathbf{u}}(i,j)}\right]\mathbb{E}\left[\left(g_{ij}g_{ij}^*\right)^{\phi_{\mathbf{u}}(i,j)}\right] \cdot \mathbb{E}\left[\mathcal{P}\left(\left\{g_{i'j'}, g_{i'j'}^*, \beta_{i'j'}\right\}_{i',j' \in \mathbb{N}, (i',j') \neq (i,j)}, \beta_{ij}\right)\right],$$

where $\mathcal{P}$ denotes arbitrary polynomial function. Since $\mathbb{E}\left[g_{ij}^{\psi_{\mathbf{u}}(i,j)-\phi_{\mathbf{u}}(i,j)}\right] = 0$ for its circular symmetric property, it results in $\Pi(\mathbf{H}, \mathbf{u}) = 0$. Same result can be easily derived for the case of $\psi_{\mathbf{u}}(i,j) - \phi_{\mathbf{u}}(i,j) < 0$ by exploiting the symmetricity. □

For the sequences except nil sequences, we have devised so-called *alphabet sequence naming convention* to classify the sequences into subgroups and labeling the subgroups according to the way how the sequences are constructed. Note that sequences included in same subgroup obviously have identical $\Pi(\mathbf{H}, \mathbf{u})$ value that they fall in the same group; however, two or more subgroups may result in identical $\Pi(\mathbf{H}, \mathbf{u})$ that those subgroups merge into the same sequence group. The details of naming convention are introduced in the following.

Let us begin with the chain product $\mathcal{E}(\mathbf{H}, \mathbf{u}, k)$ in the form of fully unfolded chain product that

$$\mathcal{E}(\mathbf{H}, \mathbf{u}, k) = h_{i_1 j_1} h_{i_2 j_1}^* h_{i_2 j_2} h_{i_3 j_2}^* \cdots h_{i_k j_k} h_{i_{k+1} j_k}^*. \tag{10}$$

From the first element on the right hand side, each element is marked by corresponding alphabet. If the element nor its conjugate has not been presented in the previous elements, the element is marked by new uppercase letter with alphabetical order. If the element has been presented in any of the previous elements, the element is marked by the identical letter given in the previous appearance. If the conjugate of the element has been ever presented in any of the previous elements, the element gets the lowercase version of the letter granted in the appearance of its conjugate.

For instance, let us consider the sequence with $k = 4$, which has two distinct row indices $i_1 (= i_4, i_5), i_2 (= i_3)$ and two distinct column indices $j_1 (= j_2, j_3), j_4$. Following the above naming convention, the sequence $\mathbf{u}$ named and included in the group for "ABbBbaCc," which can be translated from $h_{i_1 j_1} h_{i_2 j_1}^* h_{i_2 j_1} h_{i_2 j_1}^* h_{i_2 j_1} h_{i_1 j_1}^* h_{i_1 j_4} h_{i_1 j_4}^*$. As another example, let us consider the sequence with $k = 4$, which has two distinct row indices $i_1 (= i_2 = i_5), i_3 (= i_4)$ and three distinct column indices $j_1, j_2 (= j_4), j_3$. The sequence shall be included in the group named "AaBCDdcb," which is translated from $h_{i_1 j_1} h_{i_1 j_1}^* h_{i_1 j_2} h_{i_3 j_2}^* h_{i_3 j_3} h_{i_3 j_3}^* h_{i_3 j_4} h_{i_1 j_2}^*$.

Graphical representation for two examples is given above in Figure 1 for better understanding of the naming convention. Red and blue vertices are indicating row and column indices, respectively, and arrows are drawn to describe a traversal in each graph. For example, the graph depicted in Figure 1A shows a traversal passing $i_1, j_1, i_2, j_1, i_2, j_1, i_1, j_4, i_1$ sequentially to represent the sequences in group "ABbBbaCc."

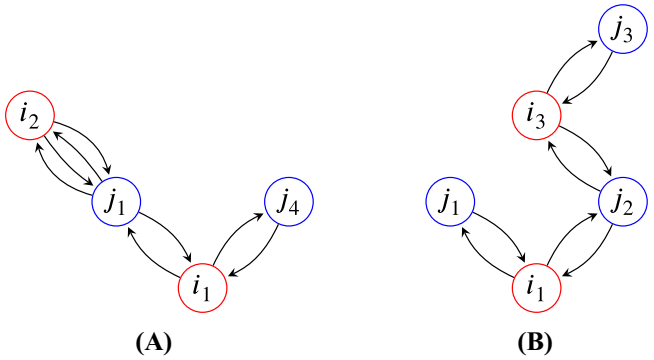

FIGURE 1 Graphical representation of the naming convention for example sequences. (A) ABbBbaCc and (B) AaBCDdcb.

3.3 | Analysis on moments of eigenvalues

In order to derive analytic solutions for moments described in (8), divide-and-conquer strategy has been exploited. First, the calculation of $\Pi(\mathbf{H}, \mathbf{u})$ value, which is identical within a sequence group, is of concern. Since the nil sequences only bear value of zero that contribute none to the summation, we take $\psi_{\mathbf{u}}(i,j) = \phi_{\mathbf{u}}(i,j)$ as a basic property in further description for all sequences but nil sequences, because every sequence other than nil sequences necessarily meets this property. From the definition of $\Pi(\mathbf{H}, \mathbf{u})$ and (9), we obtain

$$\begin{aligned}\Pi(\mathbf{H},\mathbf{u}) &= \prod_{(i,j)} \mathbb{E}\left[\left(h_{ij}h_{ij}^*\right)^{\psi_{\mathbf{u}}(i,j)}\right] \\ &= \prod_{(i,j)} \mathbb{E}\left[\left(g_{ij}g_{ij}^*\right)^{\psi_{\mathbf{u}}(i,j)}\right] \mathbb{E}\left[\left(\beta_{ij}\right)^{2\psi_{\mathbf{u}}(i,j)}\right] \\ &= \prod_{(i,j)} \psi_{\mathbf{u}}(i,j)!\,\mathbb{E}\left[\left(\beta_{ij}\right)^{2\psi_{\mathbf{u}}(i,j)}\right],\end{aligned} \tag{11}$$

where the proof of the last equality is provided in reference of eq. (6) in [11].

Denote $\mathcal{G}^k$ be set of all sequence subgroups, which can be represented by alphabet sequence with length $2k$. And for its arbitrary member sequence subgroup $\Xi \in \mathcal{G}^k$, let I_Ξ and J_Ξ, respectively, to be the number of distinct row indices and the number of distinct column indices. The kth moment of λ_n can be derived from (8) that

$$\begin{aligned}\mu_k &= \sum_{\substack{\mathbf{u}\in\mathbb{N}^{2k+1} \\ u_1 = u_{2k+1} = i'_1}} \Pi(\mathbf{H},\mathbf{u}) \\ &= \sum\nolimits_{\Xi\in\mathcal{G}^k} \underbrace{\sum_{i'_2}\cdots\sum_{i'_{I_\Xi}}}_{I_\Xi - 1} \underbrace{\sum_{j'_1}\cdots\sum_{j'_{J_\Xi}}}_{J_\Xi} \Pi(\mathbf{H},\mathbf{u}_\Xi),\end{aligned} \tag{12}$$

where $i'_1, \ldots, i'_{I_\Xi}$ are renumbered row indices, $j'_1, \ldots, j'_{J_\Xi}$ are renumbered column indices, and $\mathbf{u}_\Xi$ is a typical index sequence from subgroup Ξ.

While combining the results of (11) and (12), Campbell's theorem plays significant role in summing up the chain product expectations.

Theorem 1 (Campbell's theorem). When a point process Φ is defined over $\mathbb{R}^d$ with intensity $\Lambda(\cdot)$, arbitrary measurable function $f: \mathbb{R}^d \to \mathbb{R}$ follows an equality that

$$\mathbb{E}\left[\sum_{\mathbf{x}\in\Phi} f(\mathbf{x})\right] = \int_{\mathbb{R}^d} f(\mathbf{x})\Lambda(\mathrm{d}\mathbf{x}).$$

By applying Campbell's theorem, we can obtain the relations that

$$\begin{aligned}\mathbb{E}\left[\sum_i \beta_{ij}^n\right] &= \mathbb{E}\left[\sum_{\mathbf{q}_i\in\Phi_\mathrm{r}} L^n\left(\left|\mathbf{p}_j - \mathbf{q}_i\right|\right)\right] \\ &= \int_{\mathbb{R}^2} L^n(|\mathbf{x}|)\rho_\mathrm{r}\mathrm{d}\mathbf{x} = \int_0^\infty L^n(r)2\pi r\rho_\mathrm{r}\mathrm{d}r\end{aligned} \tag{13}$$

and

$$\begin{aligned}\mathbb{E}\left[\sum_j \beta_{ij}^n\right] &= \mathbb{E}\left[\sum_{\mathbf{p}_j\in\Phi_\mathrm{t}} L^n\left(\left|\mathbf{p}_j - \mathbf{q}_i\right|\right)\right] \\ &= \int_{\mathbb{R}^2} L^n(|\mathbf{x}|)\rho_\mathrm{t}\mathrm{d}\mathbf{x} = \int_0^\infty L^n(r)2\pi r\rho_\mathrm{t}\mathrm{d}r.\end{aligned} \tag{14}$$

It is noteworthy that the results have independency to the position of the reference point in the summation, and this origin independence property comes from the homogeneity of those PPPs.

Theorem 2 (Moments of DAS-to-DAS System Channel Eigenvalues). The kth moment of channel eigenvalues for DAS-to-DAS system with given transmit and receive node density, ρ_t and ρ_r, can be obtained by following equation that

$$\mu_k = \sum_{\Xi\in\mathcal{G}^k} \rho_\mathrm{r}^{I_\Xi - 1}\rho_\mathrm{t}^{J_\Xi} \prod_{\substack{(i,j) \\ \psi_{\mathbf{u}}(i,j)\neq 0}} \zeta_{\psi_{\mathbf{u}}(i,j)}, \tag{15}$$

where $\zeta_n = n!\int_0^\infty L^{2n}(r)2\pi r\mathrm{d}r$ (for $n \in \mathbb{N}$).

Proof. Combine the results of (11) and (12) and using commutability of summation and expectation to form

$$\begin{aligned}\mu_k = \sum_{\Xi\in\mathcal{G}^k} &\prod_{m=2}^{I_\Xi} \mathbb{E}\left[\sum_{i'_m} \psi_{\mathbf{u}}(i'_m,j)!\left(\beta_{i'_m j}\right)^{2\psi_{\mathbf{u}}(i'_m,j)}\right] \\ &\prod_{n=1}^{J_\Xi} \mathbb{E}\left[\sum_{j'_n} \psi_{\mathbf{u}}(i,j'_n)!\left(\beta_{ij'_n}\right)^{2\psi_{\mathbf{u}}(i,j'_n)}\right]\end{aligned} \tag{16}$$

and apply the relation of (13) and (14) for $I_\Xi - 1$ times and J_Ξ times, respectively.[†] □

3.4 | Sequence subgroup discovery algorithm

In order to conduct the summation over all the sequence subgroups in (15), the whole set of sequence groups should be specified for given k. The problem of finding all sequence groups can be expressed in language of combinatorics and graph theory that *classifying traversals on trees in bipartite graph* problem. To tackle this problem, a path finding algorithm is proposed, and its pseudocode is described in Algorithm 1. The algorithm operates in recursive way to perform exhaustive search of sequence subgroups. And each move of those traversal follows the scheme described in Algorithm 2.[‡]

Algorithm 1 Path finding algorithm

```
procedure PATHFINDER-INITIALIZER()
    G.v_curr ← 1
    G.v_curr.color ← RED
    G.seq ← []
    G.lifetime ← k
end procedure
procedure PATHFINDER(G)
    if G.lifetime = 0 & G.v_curr = 1 then
        (I, J) = countRedAndBlue(G)
        record(G.seq, I, J)
    else
        if G.lifetime ≠ 0 then
            for ∀v_next connected to G.v_curr do
                G' = MOVE(G, v_next)
                PATHFINDER(G')
            end for
            G' = MOVE(G, G.v_max + 1)
            PATHFINDER(G')
        else
            G' = MOVE(G, G.v_prev)
            PATHFINDER(G')
        end if
    end if
end procedure
```

4 | ANALYTIC SOLUTION AND SIMULATION RESULTS

The exhaustive search on subgroups of index sequence is conducted for $k = 1, 8$ and part of the list for sequence groups in Table A1. Consequentially, The analytic solution for the first four moments of typical channel eigenvalue is presented as

$$\begin{aligned}
\mu_1 &= \rho_t\zeta_1 \\
\mu_2 &= \rho_t\zeta_2 + (\rho_r\rho_t + \rho_t^2)\zeta_1^2 \\
\mu_3 &= \rho_t\zeta_3 + (3\rho_r\rho_t + 3\rho_t^2)\zeta_2\zeta_1 + (\rho_r^2\rho_t + 3\rho_r\rho_t^2 + \rho_t^3)\zeta_1^3 \\
\mu_4 &= \rho_t\zeta_4 + (4\rho_r\rho_t + 4\rho_t^2)\zeta_3\zeta_1 + (3\rho_r\rho_t + 3\rho_t^2)\zeta_2^2 \\
&\quad + (6\rho_r^2\rho_t + 16\rho_r\rho_t^2 + 6\rho_t^3)\zeta_2\zeta_1^2 \\
&\quad + (\rho_r^3\rho_t + 6\rho_r^2\rho_t^2 + 6\rho_r\rho_t^3 + \rho_t^4)\zeta_1^4,
\end{aligned} \tag{17}$$

and higher order moments are introduced in Appendix B. Note that the solution for $\rho_t > \rho_r$ cases can be obtained by mutually swapping ρ_t and ρ_r in (17) and Appendix B. In addition, the analytic form representations for channel model dependent terms ζ_n are presented in Table 1.

We now present concrete values of the analytic solution for moments of channel eigenvalues under specific system configuration with given system parameters. Furthermore, the results of analysis are compared with the values obtained by Monte-Carlo simulation. Since it is impossible to implement infinite plane in the simulation, the geometric simulation environment is settled as wrap-arounded rectangular domain with finite surface. Detailed simulation parameter information is given in Table 2.

The first four moments of channel eigenvalues under the circumstances described above are presented in Figure 2. The difference gap between the analytic solution and the simulation result comes from impossibility of implementing infinite number of nodes in the simulation.

5 | PER-AREA PERFORMANCE LOWER BOUND ANALYSIS OF DAS-TO-DAS

The per-area capacity of DAS to DAS can be obtained by applying water-filling power allocation algorithm to channel eigenvalues. However, the application of water-filling algorithm requires perfect knowledge on eigenvalue probability density function, which is not attainable with current knowledge. Thus, per-area performance

[†]For more rigorous proof, the indices of reference point i and j should be further specified by announcing them as indices of previous vertex immediate before of first visit to vertex of concern. However, it is possible to have the identical result by using origin independence property denoted in the previous subsection while leaving some ambiguity.

[‡]The arithmetic sequence of coefficients which can be found by forementioned two algorithms is universally applicable. Thus, once it is found it does not require to be found repeatedly over different channel models or environmental parameters.

Algorithm 2 Inter-vertex moving algorithm

procedure $\mathcal{G}'$ =MOVE($\mathcal{G}, v_{next}$)
  $\mathcal{G}' \leftarrow \mathcal{G}$
  if $v_{next} > \mathcal{G}'.v_{max}$ **then**
    if $\mathcal{G}'.v_{curr}$.color = RED **then**
      $\mathcal{G}'.v_{next}$.color = BLUE
    else
      $\mathcal{G}'.v_{next}$.color = RED
    end if
    $e \leftarrow (v_{curr}, v_{next})$
    $e' \leftarrow (v_{next}, v_{curr})$
    e.name $\leftarrow$ getNewUpperCase()
    e'.name $\leftarrow$ getLowerCase(e)
    $\mathcal{G}'$.seq.append(e.name)
    $\mathcal{G}'.v_{curr}.\mathcal{E}$.addEdge(getNewUpperCase())
    $\mathcal{G}'.v_{next}.\mathcal{E}$.addEdge(getNewLowerCase())
    $\mathcal{G}'$.lifetime $\leftarrow \mathcal{G}$.lifetime $- 1$
    $\mathcal{G}'.v_{curr} \leftarrow v_{next}$
    $\mathcal{G}'.v_{max} \leftarrow \mathcal{G}.v_{max} + 1$
  else
    $e \leftarrow (v_{curr}, v_{next})$
    $\mathcal{G}'$.seq.append(e.name)
    if IsUpperCase($\mathcal{G}'$.seq.append(e.name)) **then**
      $\mathcal{G}'$.lifetime $\leftarrow \mathcal{G}$.lifetime $- 1$
    end if
    $\mathcal{G}'.v_{curr} \leftarrow v_{next}$
  end if
end procedure

TABLE 1 Values of ζ_n by pathloss type.

Pathloss type	$L(d)$	ζ_n
MSPM	$\sqrt{c_0}\max(d, d_0)^{-\alpha/2}$	$\pi d_0^2 \left(c_0 d_0^{-\alpha}\right)^n \left(1 + \frac{2}{\alpha n - 2}\right)$
VEPM	$\sqrt{c_0}\sqrt{h_0^2 + d^2}^{-\alpha/2}$	$\frac{2\pi}{\alpha n - 2} c_0^n h_0^{2-\alpha n}$

TABLE 2 Simulation parameters for Monte-Carlo simulation.

Attributes	Value
Domain of node distribution	Rectangular, 100 m × 100 m
# of transmitter nodes	500 (fixed, $\rho_t = 0.05$ nodes/m^2)
# of receiver nodes	250, 500, 750, 1000 ($\rho_r = 0.025$, 0.05, 0.075, 0.1 nodes/m^2)
# of iterations	1000 by each
Pathloss model	MSPM ($c_0 = 10$, $d_0 = 1$ m, $\alpha = 3$) VEPM ($c_0 = 10$, $h_0 = 1$ m, $\alpha = 3$)

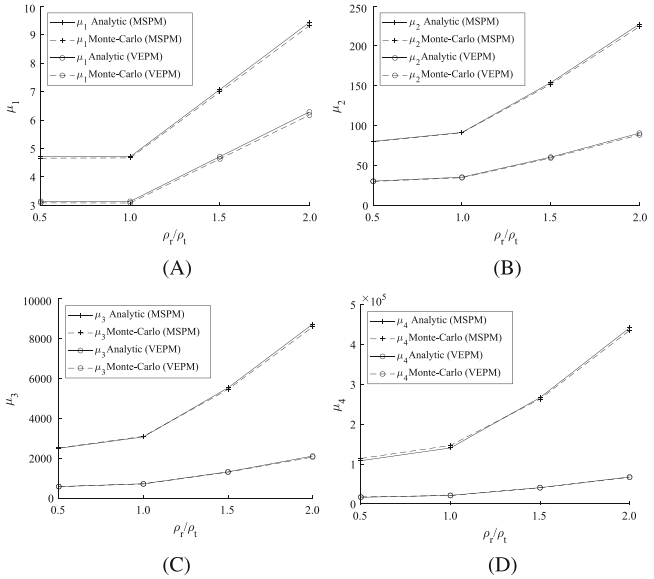

FIGURE 2 Analytic solution and Monte-Carlo simulation results for (A) μ_1, (B) μ_2, (C) μ_3, and (D) μ_4.

lower bound analysis has been conducted with partial knowledge of eigenvalue distribution by using Chebyshev's inquality. The Chebyshev's inequaility for random variable λ with mean $\mathbb{E}[\lambda] = \mu_1$ and standard deviation $\sigma[\lambda] = \sqrt{\mu_2 - \mu_1^2}$ is described as

$$P\left[|\lambda - \mu_1| \geq k\sqrt{\mu_2 - \mu_1^2}\right] \leq \frac{1}{k^2}, \tag{18}$$

and the inequality is useful for arbitrary $k > 1$.

The inequality can be rewritten in the form that guaranteeing specific probability (i.e., 0.75 for $k = 2$ case) of λ being above minimum value.

$$P\left[\lambda \geq \mu_1 - k\sqrt{\mu_2 - \mu_1^2}\right] \geq 1 - \frac{1}{k^2}. \tag{19}$$

Since the dimension of channel matrix is doubly infinite, the number of eigenvalues is also infinite. However, the number of eigenvalues per area can be described in finite form $\rho_e = \min(\rho_t, \rho_r)$. Let the MIMO system describing equation for DAS to DAS be as

$$\mathbf{y} = \mathbf{H}\mathbf{x} + \mathbf{n}, \tag{20}$$

where $\mathbf{x}, \mathbf{y}, \mathbf{n} \in \mathbb{C}^{\infty \times 1}$. And the transmit power is defined as $\mathbb{E}[\mathbf{x}\mathbf{x}^H] = P\mathbf{I}$ with per-transmitter transmit power P and the noise characteristics are defined as $\mathbb{E}[\mathbf{n}\mathbf{n}^H] = N\mathbf{I}$ with per-receiver received noise power N.

The lower bound for per-area capacity of DAS to DAS can be calculated as

$$\begin{aligned}\frac{C}{A} &= \frac{1}{A}\log\left(\mathbf{I}+\frac{P}{N}\mathbf{H}\boldsymbol{\Sigma}\mathbf{H}^{H}\right)\\ &= \frac{1}{A}\sum_{n}\log\left(1+\frac{P}{N}\lambda_n\right)\\ &= \rho_e\mathbb{E}\left[\log\left(1+\frac{P}{N}\lambda\right)\right]\\ &\geq \max_{k}\left(1-\frac{1}{k^2}\right)\rho_e\log\left(1+\frac{P}{N}\left(\mu_1-k\sqrt{\mu_2-\mu_1^2}\right)\right),\end{aligned} \tag{21}$$

where $\boldsymbol{\Sigma}$ is channel orthogonalizing precoding matrix and A is the surface area of infinite terrain with little abuse of notation.

6 | CONCLUSION

In this paper, we modeled MIMO communication system between two groups of geometrically distributed nodes equipped with single antenna, namely, DAS-to-DAS system. Each entry of the MIMO channel random matrix is modeled with non-singular pathloss models and Rayleigh fading coefficient. The equality between channel eigenvalue moment of arbitrary order and expectation of a diagonal entry in Gramian matrix powered by identical order had shown for further improvision. Since the value of moment is represented in the form of summation of channel matrix entries' chain product, we classified the chain products into several groups by identical expectation values. A naming convention for such groups has suggested and a method of calculating expectation of chain product has introduced. With the aid of Campbell's theorem, analytic solution for the first a few moments of channel eigenvalue is derived in closed form. The results of analysis were shown to conform with the results of Monte-Carlo simulation performed over finite domain of node distribution.

The plan for future work is as following. First, we will expand the attained analytic solution for channel eigenvalue moments to all order to obtain exact profile of moment generating function. Then, we will convert the moment generating function into probability density function of the eigenvalues. Finally, we will derive values for performance metrics with the knowledge of channel eigenvalue distribution under DAS-to-DAS system configuration.

CONFLICT OF INTEREST

The authors declare no potential conflict of interest.

ORCID

Donghyuk Gwak https://orcid.org/0000-0002-1436-0336

REFERENCES

1. A. AlAmmouri, J. G. Andrews, and F. Baccelli, *Scaling laws of dense multi-antenna cellular networks*, (54th Asilomar Conference on Signals, Systems, and Computers, Pacific Grove, CA, USA), 2020, pp. 1041–1045.
2. J. Park, J. P. Hong, W. Shin, and S. Kim, *Performance analysis of distributed antenna system for downlink ultrareliable low-latency communications*, IEEE Syst. J. **15** (2020), no. 1, 518–525.
3. A. Guo, Y. Zhong, W. Zhang, and M. Haenggi, *The Gauss-Poisson process for wireless networks and the benefits of cooperation*, IEEE Trans. Commun. **64** (2016), no. 5, 1916–1927.
4. C. Zhang, Y. Liu, and Z. Ding, *Semi-grant-free NOMA: a stochastic geometry model*, IEEE Trans. Wirel. Commun. **21** (2022), no. 2, 1197–1213.
5. L. A. Pastur and V. A. Marchenko, *The distribution of eigenvalues in certain sets of random matrices*, Math. USSR-Sbornik **1** (1967), no. 4, 457–483.
6. M. Chianni, M. Z. Win, and A. Zanella, *On the capacity of spatially correlated MIMO Rayleigh-fading channels*, IEEE Trans. Inform. Theory **49** (2003), no. 10, 2363–2371.
7. C. Martin and B. Ottersten, *Asymptotic eigenvalue distributions and capacity for MIMO channels under correlated fading*, IEEE Trans. Wirel. Commun. **3** (2004), no. 4, 1350–1359.
8. G. Alfano, A. Lozano, A. M. Tulino, and S. Verdú, *Mutual information and eigenvalue distribution of MIMO Ricean channels*, (IEEE International Symposium on Information Theory and its Applications, Parma, Italy), 2009, pp. 1–6.
9. D. Tsilimantos, J. M. Gorce and E. Altman, *Stochastic analysis of energy savings with sleep mode in OFDMA wireless networks*, (Proceedings IEEE INFOCOM, Turin, Italy), 2013, pp. 1097–1105.
10. M. Banagar and H. S. Dhillon, *3GPP-inspired stochastic geometry-based mobility model for a drone cellular network*, (IEEE Global Communications Conference, Waikoloa, HI, USA), 2019, pp. 1–6.
11. C. Fassino, G. Pistone, and M. P. Rogantin, *Computing the moments of the complex Gaussian: full and sparse covariance matrix*, Math. **7** (2019), no. 3, 263–280.

AUTHOR BIOGRAPHIES

Donghyuk Gwak received the BS and MS degrees in the field of electrical engineering from Seoul National University, Republic of Korea, in 2010 and 2013, respectively. He has been with the Electronics and Telecommunications Research Institute, Daejeon, Republic of Korea since 2013. His research interests include MIMO, random matrix theory, DAS, and heterogeneous network.

Youngil Jeon received the BS and MS degrees in Electrical Engineering from Korea University, Seoul, Republic of Korea, in 2010 and 2012, respectively. Since 2012, he has been with the Electronics and Telecommunications Research Institute, Daejeon, Republic of Korea, as a research engineer. His research interests include the 3GPP 5G NR systems, information theory, and signal processing for wireless and satellite communications.

Jemin Lee received the BS (with high honors), MS, and PhD degrees in Electrical and Electronic Engineering from Yonsei University, Seoul, Republic of Korea, in 2004, 2007, and 2010, respectively. She was a postdoctoral fellow at the Massachusetts Institute of Technology (MIT), Cambridge, MA, USA, from 2010 to 2013; a Temasek Research Fellow at iTrust, Centre for Research in Cyber Security, Singapore University of Technology and Design (SUTD), Singapore, from 2014 to 2016; an associate professor at the Department of Information and Communication Engineering, Daegu Gyeongbuk Institute of Science and Technology (DGIST), Daegu, Republic of Korea, from 2016 to 2021; and an associate professor at the Department of Electrical and Computer Engineering, Sungkyunkwan University (SKKU), Suwon, Republic of Korea, from 2021 to 2023. Currently, she is an associate professor at the School of Electrical and Electronic Engineering, Yonsei University, Seoul, Republic of Korea. Her current research interests include wireless communications, wireless security, intelligent networking, and blockchain networks.

Jee-Hyeon Na received the BS degree in computer science from Chonnam National University, Gwangju, Republic of Korea and MS and PhD degrees in computer science from Chungnam National University, Daejeon, Republic of Korea in 2002 and 2008, respectively. She has been with Electronics and Telecommunications Research Institute, Daejeon, Republic of Korea since 1989, where she is currently the Director of the Intelligent Small Cell Research Section. Her research interests are in the area of 5G small cells, Self-Organizing Network (SON), and location management and paging for mobile communication networks. She is a member of IEICE communication part and IEEE.

How to cite this article: D. Gwak, Y. Jeon, J. Lee, and J.-H. Na, *Moment analysis on channel eigenvalue for DAS-to-DAS system*, ETRI Journal **47** (2025), 69–79, DOI 10.4218/etrij.2023-0367.

APPENDIX A: A LIST OF INDEX SEQUENCE GROUPS

TABLE A1 Classification of index sequence groups.

	Group name	ψ_u sorted in Descending order	(I_Ξ, J_Ξ)
$k = 1$	Aa	[1, 0]	(1, 1)
$k = 2$	AaAa	[2, 0]	(1, 1)
	AaBb	[1]	(1, 2)
	ABba	[1]	(2, 1)
$k = 3$	AaAaAa	[3, 0, 0]	(1, 1)
	AaAaBb	[2, 1, 0]	(1, 2)
	AaABba	[2, 1, 0]	(2, 1)
	AaBbAa	[2, 1, 0]	(1, 2)
	AaBbBb	[2, 1, 0]	(1, 2)
	AaBbCc	[1]	(1, 3)
	AaBCcb	[1]	(2, 2)
	ABbaAa	[2, 1, 0]	(2, 1)
	ABbaCc	[1]	(2, 2)
	ABbBba	[2, 1, 0]	(2, 1)
	ABbCca	[1]	(3, 1)
k = 3	ABCcba	[1]	(2, 2)
k = 4	AaAaAaAa	[4, 0, 0, 0]	(1, 1)
	AaAaAaBb	[3, 1, 0, 0]	(1, 2)
	AaAaABba	[3, 1, 0, 0]	(2, 1)
	AaAaBbAa	[3, 1, 0, 0]	(1, 2)
	AaAaBbBb	[2, 2, 0, 0]	(1, 2)
	AaAaBbCc	[2, 1, 1, 0]	(1, 3)
	AaAaBCcb	[2, 1, 1, 0]	(2, 2)
	AaABbaAa	[3, 1, 0, 0]	(2, 1)
	AaABbaCc	[2, 1, 1, 0]	(2, 2)
	AaABbBba	[2, 2, 0, 0]	(2, 1)
	AaABbCca	[2, 1, 1, 0]	(3, 1)
	AaABCcba	[2, 1, 1, 0]	(2, 2)
	AaBbAaAa	[3, 1, 0, 0]	(1, 2)
	AaBbAaBb	[2, 2, 0, 0]	(1, 2)
	AaBbAaCc	[2, 1, 1, 0]	(1, 3)
	AaBbACca	[2, 1, 1, 0]	(2, 2)
	AaBbBbAa	[2, 2, 0, 0]	(1, 2)
	AaBbBbBb	[3, 1, 0, 0]	(1, 2)
	AaBbBbCc	[2, 1, 1, 0]	(1, 3)
	AaBbBCcb	[2, 1, 1, 0]	(2, 2)
	AaBbCcAa	[2, 1, 1, 0]	(1, 3)
	AaBbCcBb	[2, 1, 1, 0]	(1, 3)
	AaBbCcCc	[2, 1, 1, 0]	(1, 3)
	AaBbCcDd	[1]	(1, 4)
	AaBbCDdc	[1]	(2, 3)
	AaBCcbAa	[2, 1, 1, 0]	(2, 2)
	AaBCcbBb	[2, 1, 1, 0]	(2, 2)
	AaBCcbDd	[1]	(2, 3)
	AaBCcCcb	[2, 1, 1, 0]	(2, 2)
	AaBCcDdb	[1]	(3, 2)
	AaBCDdcb	[1]	(2, 3)
	ABbaAaAa	[3, 1, 0, 0]	(2, 1)
	ABbaAaCc	[2, 1, 1, 0]	(2, 2)
	ABbaABba	[2, 2, 0, 0]	(2, 1)
	ABbaACca	[2, 1, 1, 0]	(3, 1)
	ABbaCcAa	[2, 1, 1, 0]	(2, 2)
	ABbaCcCc	[2, 1, 1, 0]	(2, 2)
	ABbaCcDd	[1]	(2, 3)
	ABbaCDdc	[1]	(3, 2)
	ABbBbaAa	[2, 2, 0, 0]	(2, 1)
	ABbBbaCc	[2, 1, 1, 0]	(2, 2)
	ABbBbBba	[3, 1, 0, 0]	(2, 1)
	ABbBbCca	[2, 1, 1, 0]	(3, 1)
	ABbBCcba	[2, 1, 1, 0]	(2, 2)
	ABbCcaAa	[2, 1, 1, 0]	(3, 1)
	ABbCcaDd	[1]	(3, 2)
	ABbCcBba	[2, 1, 1, 0]	(3, 1)
	ABbCcCca	[2, 1, 1, 0]	(3, 1)
	ABbCcDda	[1]	(4, 1)
	ABbCDdca	[1]	(3, 2)
k = 4	ABCcbaAa	[2, 1, 1, 0]	(2, 2)
	ABCcbaDd	[1]	(2, 3)
	ABCcbBba	[2, 1, 1, 0]	(2, 2)
	ABCcbDda	[1]	(3, 2)
	ABCcCcba	[2, 1, 1, 0]	(2, 2)
	ABCcDdba	[1]	(2, 3)
	ABCDdcba	[1]	(3, 2)

APPENDIX B: HIGHER ORDER MOMENTS

$$
\begin{aligned}
\mu_5 = {} & \rho_t\zeta_5 + \left(5\rho_r\rho_t + 5\rho_t^2\right)\zeta_4\zeta_1 + \left(10\rho_r\rho_t + 10\rho_t^2\right)\zeta_3\zeta_2 \\
& + \left(10\rho_r^2\rho_t + 25\rho_r\rho_t^2 + 10\rho_t^3\right)\zeta_3\zeta_1^2 \\
& + \left(15\rho_r^2\rho_t + 35\rho_r\rho_t^2 + 15\rho_t^3\right)\zeta_2^2\zeta_1 \\
& + \left(10\rho_r^3\rho_t + 50\rho_r^2\rho_t^2 + 50\rho_r\rho_t^3 + 10\rho_t^4\right)\zeta_2\zeta_1^3 \\
& + \left(\rho_r^4\rho_t + 10\rho_r^3\rho_t^2 + 20\rho_r^2\rho_t^3 + 10\rho_r\rho_t^4 + \rho_t^5\right)\zeta_1^5 \\
\mu_6 = {} & \rho_t\zeta_6 + \left(6\rho_r\rho_t + 6\rho_t^2\right)\zeta_5\zeta_1 + \left(15\rho_r\rho_t + 15\rho_t^2\right)\zeta_4\zeta_2 \\
& + \left(15\rho_r^2\rho_t + 36\rho_r\rho_t^2 + 15\rho_t^3\right)\zeta_4\zeta_1^2 \\
& + \left(10\rho_r\rho_t + 10\rho_t^2\right)\zeta_3^2 \\
& + \left(60\rho_r^2\rho_t + 132\rho_r\rho_t^2 + 60\rho_t^3\right)\zeta_3\zeta_2\zeta_1 \\
& + \left(20\rho_r^3\rho_t + 90\rho_r^2\rho_t^2 + 90\rho_r\rho_t^3 + 20\rho_t^4\right)\zeta_3\zeta_1^3 \\
& + \left(15\rho_r^2\rho_t + 27\rho_r\rho_t^2 + 15\rho_t^3\right)\zeta_2^3 \\
& + \left(45\rho_r^3\rho_t + 186\rho_r^2\rho_t^2 + 186\rho_r\rho_t^3 + 45\rho_t^4\right)\zeta_2^2\zeta_1^2 \\
& + \left(15\rho_r^4\rho_t + 120\rho_r^3\rho_t^2 + 225\rho_r^2\rho_t^3 + 120\rho_r\rho_t^4 + 15\rho_t^5\right)\zeta_2\zeta_1^4 \\
& + \left(\rho_r^5\rho_t + 15\rho_r^4\rho_t^2 + 50\rho_r^3\rho_t^3 + 50\rho_r^2\rho_t^4 + 15\rho_r\rho_t^5 + \rho_t^6\right)\zeta_1^6 \\
\mu_7 = {} & \rho_t\zeta_7 + \left(7\rho_r\rho_t + 7\rho_t^2\right)\zeta_6\zeta_1 + \left(21\rho_r\rho_t + 21\rho_t^2\right)\zeta_5\zeta_2 \\
& + \left(21\rho_r^2\rho_t + 49\rho_r\rho_t^2 + 21\rho_t^3\right)\zeta_5\zeta_1^2 \\
& + \left(35\rho_r\rho_t + 35\rho_t^2\right)\zeta_4\zeta_3 \\
& + \left(105\rho_r^2\rho_t + 224\rho_r\rho_t^2 + 105\rho_t^3\right)\zeta_4\zeta_2\zeta_1 \\
& + \left(35\rho_r^3\rho_t + 147\rho_r^2\rho_t^2 + 147\rho_r\rho_t^3 + 35\rho_t^4\right)\zeta_4\zeta_1^3 \\
& + \left(70\rho_r^2\rho_t + 147\rho_r\rho_t^2 + 70\rho_t^3\right)\zeta_3^2\zeta_1 \\
& + \left(105\rho_r^2\rho_t + 168\rho_r\rho_t^2 + 105\rho_t^3\right)\zeta_3\zeta_2^2 \\
& + \left(210\rho_r^3\rho_t + 791\rho_r^2\rho_t^2 + 791\rho_r\rho_t^3 + 210\rho_t^4\right)\zeta_3\zeta_2\zeta_1^2 \\
& + \left(35\rho_r^4\rho_t + 245\rho_r^3\rho_t^2 + 441\rho_r^2\rho_t^3 + 245\rho_r\rho_t^4 + 35\rho_t^5\right)\zeta_3\zeta_1^4 \\
& + \left(105\rho_r^3\rho_t + 336\rho_r^2\rho_t^2 + 336\rho_r\rho_t^3 + 105\rho_t^4\right)\zeta_2^3\zeta_1 \\
& + \left(105\rho_r^4\rho_t + 672\rho_r^3\rho_t^2 + 1176\rho_r^2\rho_t^3 + 672\rho_r\rho_t^4 + 105\rho_t^5\right)\zeta_3\zeta_1^4 \\
& + \left(21\rho_r^5\rho_t + 245\rho_r^4\rho_t^2 + 735\rho_r^3\rho_t^3 + 735\rho_r^2\rho_t^4 + 245\rho_r\rho_t^5 + 21\rho_t^6\right)\zeta_2\zeta_1^5 \\
& + \left(\rho_r^6\rho_t + 21\rho_r^5\rho_t^2 + 105\rho_r^4\rho_t^3 + 175\rho_r^3\rho_t^4 + 105\rho_r^2\rho_t^5 + 21\rho_r\rho_t^6 + \rho_t^7\right)\zeta_1^7 \\
\mu_8 = {} & \rho_t\zeta_8 + \left(8\rho_r\rho_t + 8\rho_t^2\right)\zeta_7\zeta_1 + \left(28\rho_r\rho_t + 28\rho_t^2\right)\zeta_6\zeta_2 \\
& + \left(28\rho_r^2\rho_t + 64\rho_r\rho_t^2 + 28\rho_t^3\right)\zeta_6\zeta_1^2 \\
& + \left(56\rho_r\rho_t + 56\rho_t^2\right)\zeta_5\zeta_3 \\
& + \left(168\rho_r^2\rho_t + 352\rho_r\rho_t^2 + 168\rho_t^3\right)\zeta_5\zeta_2\zeta_1 \\
& + \left(56\rho_r^3\rho_t + 224\rho_r^2\rho_t^2 + 224\rho_r\rho_t^3 + 56\rho_t^4\right)\zeta_5\zeta_1^3 \\
& + \left(35\rho_r\rho_t + 35\rho_t^2\right)\zeta_4^2 \\
& + \left(280\rho_r^2\rho_t + 576\rho_r\rho_t^2 + 280\rho_t^3\right)\zeta_4\zeta_3\zeta_1 \\
& + \left(210\rho_r^2\rho_t + 320\rho_r\rho_t^2 + 210\rho_t^3\right)\zeta_4\zeta_2^2 \\
& + \left(420\rho_r^3\rho_t + 1500\rho_r^2\rho_t^2 + 1500\rho_r\rho_t^3 + 420\rho_t^4\right)\zeta_4\zeta_2\zeta_1^2 \\
& + \left(70\rho_r^4\rho_t + 448\rho_r^3\rho_t^2 + 784\rho_r^2\rho_t^3 + 448\rho_r\rho_t^4 + 70\rho_t^5\right)\zeta_4\zeta_1^4 \\
& + \left(280\rho_r^2\rho_t + 384\rho_r\rho_t^2 + 280\rho_t^3\right)\zeta_3^2\zeta_2 \\
& + \left(280\rho_r^3\rho_t + 980\rho_r^2\rho_t^2 + 980\rho_r\rho_t^3 + 280\rho_t^4\right)\zeta_3^2\zeta_1^2 \\
& + \left(840\rho_r^3\rho_t + 2392\rho_r^2\rho_t^2 + 2392\rho_r\rho_t^3 + 840\rho_t^4\right)\zeta_3\zeta_2^2\zeta_1 \\
& + \left(560\rho_r^4\rho_t + 3192\rho_r^3\rho_t^2 + 5376\rho_r^2\rho_t^3 + 3192\rho_r\rho_t^4 + 560\rho_t^5\right)\zeta_3\zeta_2\zeta_1^3 \\
& + \left(56\rho_r^5\rho_t + 560\rho_r^4\rho_t^2 + 1568\rho_r^3\rho_t^3 + 1568\rho_r^2\rho_t^4 + 560\rho_r\rho_t^5 + 56\rho_t^6\right)\zeta_3\zeta_1^5 \\
& + \left(105\rho_r^3\rho_t + 234\rho_r^2\rho_t^2 + 234\rho_r\rho_t^3 + 105\rho_t^4\right)\zeta_2^4 \\
& + \left(420\rho_r^4\rho_t + 2076\rho_r^3\rho_t^2 + 3328\rho_r^2\rho_t^3 + 2076\rho_r\rho_t^4 + 420\rho_t^5\right)\zeta_2^3\zeta_1^2 \\
& + \left(210\rho_r^5\rho_t + 1918\rho_r^4\rho_t^2 + 5152\rho_r^3\rho_t^3 + 5152\rho_r^2\rho_t^4 + 1918\rho_r\rho_t^5 + 210\rho_t^6\right)\zeta_2^2\zeta_1^4 \\
& + \left(28\rho_r^6\rho_t + 448\rho_r^5\rho_t^2 + 1960\rho_r^4\rho_t^3 + 3136\rho_r^3\rho_t^4 + 1960\rho_r^2\rho_t^5 + 448\rho_r\rho_t^6 + 28\rho_t^7\right)\zeta_2\zeta_1^6 \\
& + \left(\rho_r^7\rho_t + 28\rho_r^6\rho_t^2 + 196\rho_r^5\rho_t^3 + 490\rho_r^4\rho_t^4 + 490\rho_r^3\rho_t^5 + 196\rho_r^2\rho_t^6 + 28\rho_r\rho_t^7 + \rho_t^7\right)\zeta_1^8
\end{aligned}
$$